Available online at www.sciencedirect.com
SCIENCE DIRECT®
International Journal of Heat and Mass Transfer 48 (2005) 2771–2778
International Journal of HEAT and MASS TRANSFER
www.elsevier.com/locate/ijhmt

Transient laminar compressible boundary layers over a permeable circular cone near a plane of symmetry

M. Kumari *, G. Nath

Department of Mathematics, Indian Institute of Science, Bangalore 560012, India

Received 22 March 2004; received in revised form 15 December 2004
Available online 7 April 2005

Abstract

The transient laminar compressible boundary layer over a circular cone at an angle of attack near a plane of symmetry in hypersonic flow has been investigated. The case of the boundary layer near the windward and leeward planes has been considered. The effect of suction is included in the analysis which plays an important role in obtaining unique solution. We have examined the situation where the flow is steady at time $t = 0$ and at time $t > 0$, the total enthalpy at the wall is suddenly increased and subsequently maintained at that value. This imports unsteadiness in the flow field. The effects of the variable fluid properties, non-unity Prandtl number and viscous dissipation are considered. By suitable transformations, the coupled nonlinear parabolic partial differential equations with three independent variables governing the flow have been reduced to partial differential equations with two independent variables. The resulting partial differential equations have been solved by using an implicit finite-difference scheme in combination with the quasilinearization technique. Computations have been carried out from the initial steady state to the final steady state. It is found that in a small time interval immediately after the start of the impulsive motion, the direction of the heat transfer changes. The surface shear stresses in the streamwise and cross-wise directions and the surface heat transfer, in general, increase with time and attain final steady state values rather quickly (i.e., spin-up time is small). The total enthalpy at the wall strongly affects the surface shear stresses in the streamwise and cross-flow directions and the surface heat transfer, the suction strongly affects the surface shear stress in the streamwise direction and the surface heat transfer, and the cross-flow parameter strongly affects only the cross-flow surface shear stress.

1. Introduction

The transient three-dimensional laminar boundary layers in supersonic or hypersonic flow over a body is found in many important and interesting applications in several fields such as entry and re-entry space vehicles, accelerated or decelerated rockets and missiles, wings of supersonic aircraft. The unsteady viscous effects are found to play an important role in the stability of space vehicles and missiles. In order to predict frictional drag and the rate of heat transfer on the surface of the body for the above problems, the transient laminar compressible three-dimensional boundary layer equations governing the hypersonic or supersonic flow with four independent variables (three space variables and a time variable) have to be solved. Therefore, many research workers have considered similarity solutions while studying the three-dimensional boundary layer flows.

* Corresponding author. Tel.: +91 80 2293 3214/2265; fax: +91 80 2360 0146.
E-mail address: mkumari@math.iisc.ernet.in (M. Kumari).

0017-9310/$ - see front matter © 2005 Elsevier Ltd. All rights reserved.
doi:10.1016/j.ijheatmasstransfer.2005.01.031

Nomenclature

a	velocity of sound, m s^{-1}
A	dimensionless suction parameter = $-(3/2)^{1/2}[(\rho w)_w/(\rho u)_e]Re_x^{1/2}$
c_p	constant pressure specific heat, J kg^{-1} K
c_v	constant volume specific heat, J kg^{-1} K
Ec	viscous dissipation parameter = $u_e^2/2H_e$
f'	dimensionless velocity component along streamwise direction = u/u_e
g	dimensionless total enthalpy = H/H_e
h	specific enthalpy, J kg^{-1}
H	total enthalpy, J kg^{-1}
k	fluid thermal conductivity, W m^{-1} K
M_e	Mach number at the edge of the boundary layer = V/a
N	product of density–viscosity ratio = $\rho\mu/(\rho\mu)_e$
p	static pressure, Pa
p_0	static pressure when $\theta = 0$, Pa
p_2	denotes the curvature of the pressure distribution along the plane of symmetry, Pa
Pr	Prandtl number = $\mu_e c_p/k$
r	cylindrical radius of the cone, m
R	dimensionless function of dimensionless time $t^* = 1 + \epsilon t^{*2}$
Re_x	local Reynolds number = $u_e x/v_e$
s'	dimensionless cross-flow velocity = v/v_e
t	time, s
t^*	dimensionless time = $(3/2)(u_e/x)t$
u, v, w	velocity components along x, θ and z directions, respectively, m s^{-1}
V	fluid velocity in the inviscid flow, m s^{-1}
x	distance along a generator of the cone from apex, m
z	distance normal to the surface, m

Greek symbols

α	dimensionless cross-flow parameter = $[2\xi v_e/(\rho_e\mu_e u_e^2 r^3)]$
α_0	angle of incidence of the cone
β	dimensionless parameter associated with the three-dimensional nature of the flow = $(2\xi/v_e x)\mathrm{d}(v_e x)/\mathrm{d}\xi$
γ	specific heat ratio = c_p/c_v (1.4 for air)
$\Delta\eta$, Δt^*	dimensionless step sizes in and η and t^* directions, respectively
ϵ	dimensionless constant
η	transformed coordinate normal to the surface = $(3/2)^{1/2}(\rho_e u_e/\mu_e x)^{1/2}\int_0^\eta(\rho/\rho_e)\mathrm{d}z$
θ	circumferential angle measured from the plane of symmetry
θ_c	semi-vertical angle of the cone
μ	viscosity coefficient, kg m^{-1} s^{-1}
v	kinematic viscosity, m^2 s^{-1}
ξ	transformed streamwise coordinate = $3^{-1}\ \rho_e\mu_e u_e(\sin\theta_c)^2 x^3$
ρ	mass density, kg m^{-3}
ω	index in the power-law variation of viscosity coefficient

Subscripts

e	condition at the edge of the boundary layer
i	initial condition
w	wall condition

Superscript

$'$	prime denotes derivative with respect to η

Recently, Cousteix [1] and Betters et al. [2] have presented excellent reviews of the unsteady boundary layers. The steady compressible three-dimensional stagnation point boundary layers was investigated by Libby [3] and the corresponding unsteady case was considered by Kumari and Nath [4]. The steady laminar boundary layers over an infinite yawed circular cylinder in a supersonic flow was studied by Reshotko and Beckwith [5], whereas the corresponding unsteady case was investigated by Sau and Nath [6]. Dwyer [7] reported certain aspects of the steady three-dimensional boundary layers.

The boundary layer flow over a sharp cone near a plane of symmetry is a three-dimensional flow with pressure gradient, either favourable or adverse, and either inflow into or outflow from the plane. Such a study could be useful in the design of missiles and space vehicles. Moore [8,9] and Reshotko [10] investigated the boundary layer flow on a cone near the windward plane of symmetry, whereas Murdock [11], Roux [12], Wu and Libby [13] and Rubin et al. [14] have studied both the windward and leeward sides. These studies showed the existence of non-unique solutions in the windward and leeward plane of symmetry. A detailed study of three-dimensional compressible boundary layer flow on a cone at an angle of attack was carried out by Lin and Rubin [15]. Wortman [16] has studied the effect of injection on the laminar boundary layer flows at windward generators of sharp cones at angles of attack. He included the effects of variable fluid properties, nonunity Prandtl number and viscous dissipation in the governing equations and obtained self-similar solutions.

The above studies except [16] dealt with the self-similar solutions of the steady flows with constant fluid

properties, unit Prandtl number and without viscous dissipation. As mentioned earlier, the flow is likely to be unsteady in most problems such as entry or re-entry space vehicles which undergo deceleration, supersonic aircrafts where the speed is suddenly changed and rockets and missiles where the angle of incidence is impulsively altered. In recent years, the unsteady compressible boundary layer flow over two-dimensional and axisymmetric bodies have been investigated by a few research workers [17–19].

It is well known that suction plays an important role in controlling the boundary layer thickness. The performance criteria associated with satellites, space vehicles, aircrafts etc. significantly depend on the growth of the boundary layers. The boundary layer thickness can be considerably reduced by applying suction on the surface of the body.

This paper considers the unsteady laminar compressible three-dimensional boundary layer flow over a cone at an angle of attack near the windward and leeward sides of the plane of symmetry. The effect of suction is included in the analysis which enables us to obtain unique solution of the problem. We have considered the case where the flow is steady at time $t = 0$ and at time $t > 0$, the wall temperature is impulsively increased. This sudden increase in the wall temperature induces unsteadiness in the flow field. The effects of the variable fluid properties, non-unity Prandtl number and viscous dissipation on the flow field are considered. The flow is assumed to be axisymmetric. By suitable transformations, the unsteady compressible boundary layer equations with three independent variables have been reduced to boundary layer equations with two independent variables, The resulting system of equations has been solved numerically using an implicit finite difference scheme in combination with the quasi-linearization technique [20,21]. The computations have been carried out from the initial steady state to the final steady state. The initial steady state results in the absence of suction have been compared with those of Wu and Libby [13] and Wortman [16]. The present problem is the unsteady counterpart of the problem considered by Wu and Libby [13] and Wortman [16] and the results with suction may be useful in reducing the drag on space vehicles, missiles and aircraft.

2. Analysis

Inset of Fig. 1 shows the physical model and the coordinate system $(x, z, r\theta)$, where x is the distance along a generator of the cone from the vertex, z is the distance normal to the surface, $r(x)$ is the cylindrical radius of the cone, and θ is the circumferential angle. The corresponding velocity components are u, w and v. We consider the transient laminar compressible three-dimensional

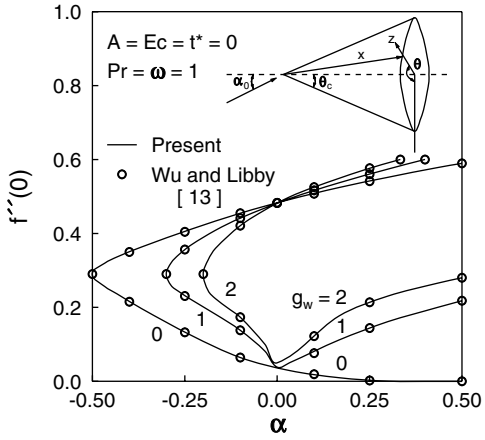

Fig. 1. Comparison of streamwise surface shear stress for the steady flow. ($f''(0)$), when $A = Ec = t^* = \epsilon = 0$, $Pr = \omega = N = 1$ with that of Wu and Libby [13].

boundary layers governing the hypersonic flow over a circular cone at an angle of incidence α_0 near a plane of symmetry. Both windward and leeward sides are considered in the analysis. We have considered the case where the flow is steady at time $t = 0$ and at time $t > 0$, the wall temperature is suddenly increased and subsequently the same wall temperature is maintained. This impulsive change imports unsteadiness in the flow field. Our aim is to study the temporal development of the flow and temperature fields starting from the initial steady state to the final steady state. We have assumed variable fluid properties and non-unity Prandtl number ($\rho \propto T^{-1}$, $\mu \propto T^{\omega}$, $Pr \neq 1$, where ρ and μ are the fluid density and viscosity, respectively, ω is the index in the power-law variation of the viscosity and Pr is the Prandtl number). The viscous dissipation term, is included in our analysis. We have taken the Prandtl number Pr to be constant in the boundary layer, because in most of the atmospheric flight problems its variation is small [22]. We have also assumed that the fluid in the inviscid flow is homentropic. Here θ is the plane of symmetry and we assume expansion for the velocity components u, v and w, total enthalpy H and static pressure p appropriate to the plane of symmetry in terms of θ (i.e., u, w, H and p even functions and v odd function). We use these expansions into the boundary layer equations for conservation of mass, momentum (x-wise and θ-wise momentum) and energy and consider only zero- and first-order terms in θ and obtain the following system of equations [13,23,24].

$$\frac{\partial}{\partial t}(\rho r) + \frac{\partial}{\partial x}(\rho u r) + \rho v + r\frac{\partial}{\partial z}(\rho w) = 0, \tag{1}$$

$$\rho\left(\frac{\partial u}{\partial t} + u\frac{\partial u}{\partial x} + w\frac{\partial u}{\partial z}\right) = -\frac{\partial p_0}{\partial x} + \frac{\partial}{\partial z}\left(\mu\frac{\partial u}{\partial z}\right), \tag{2}$$

$$\rho\left(\frac{\partial v}{\partial t}+u\frac{\partial v}{\partial x}+\frac{v^2}{r}+w\frac{\partial v}{\partial z}\right)=-\frac{2p_2}{r}+\frac{\partial}{\partial z}\left(\mu\frac{\partial v}{\partial z}\right), \tag{3}$$

$$\rho\left(\frac{\partial H}{\partial t}+u\frac{\partial H}{\partial x}+w\frac{\partial H}{\partial z}\right)=\frac{\partial p_0}{\partial t}+\frac{\partial}{\partial z}\left[\frac{\mu}{Pr}\frac{\partial H}{\partial z}+(1-Pr^{-1})\mu u\frac{\partial u}{\partial z}\right], \tag{4}$$

where

$$\begin{aligned}
&-\frac{\partial p_0}{\partial x}=\rho_e\left(\frac{\partial u_e}{\partial t}+u_e\frac{\partial u_e}{\partial x}\right),\\
&-2p_2=\rho_e v_e^2+\rho_e x\sin\theta_c\left(\frac{\partial v_e}{\partial t}+u_e\frac{\partial v_e}{\partial x}\right),\\
&\frac{\partial p_0}{\partial t}=\rho_e\left(\frac{\partial H_e}{\partial t}+u_e\frac{\partial H_e}{\partial x}\right),\\
&r=x\sin\theta_c,\quad H=h+2^{-1}u^2.
\end{aligned} \tag{5}$$

The initial conditions are given by

$$u=u_i,\quad v=v_i,\quad w=w_i,\quad H=H_i\qquad \text{at } t=0. \tag{6}$$

The boundary conditions are

$$\begin{aligned}
&u=v=0,\quad w=w_0,\quad H=H_w(1+\epsilon)\\
&\quad\text{at } z=0,\ t>0,\\
&u=u_e,\quad v=v_e,\quad H=H_e\qquad \text{as } z\to\infty,\ t>0.
\end{aligned} \tag{7}$$

Here v now denotes the velocity gradient in the direction normal to the plane of symmetry and the actual velocity either into ($v<0$) or out of ($v>0$) the plane of symmetry is $v\theta$, whereas the cross-flow velocity is given by v/v_e [13]. Since we have assumed that the fluid outside the boundary layer region (inviscid flow region) is homentropic, H_e is a constant in the inviscid flow region. Hence $\partial p_0/\partial t=0$. Also u_e and v_e are independent of time t which imply that $\partial u_e/\partial t=\partial v_e/\partial t=0$.

In order to reduce the number of independent variables from three to two as well as the number of equations from four to three, we apply the following transformations to Eqs. (1)–(4)

$$\begin{aligned}
&\eta=\left(\frac{3}{2}\frac{\rho_e u_e}{\mu_e x}\right)^{1/2}\int_0^z(\rho/\rho_e)\mathrm{d}z,\quad \xi=3^{-1}\rho_e\mu_e u_e(\sin\theta_c)^2x^3,\\
&t^*=(3/2)(u_e/x)t,\quad u(x,z,t)=u_e f'(\eta,t^*),\\
&v(x,z,t)=v_e s'(\eta,t^*),\quad H(x,z,t)=H_e g(\eta,t^*),\\
&\alpha=2\xi v_e/(\rho_e\mu_e u_e^2r^3)=(2v_e/3u_e\sin\theta_c),\\
&\beta=(2\xi/v_e x)\mathrm{d}(v_e x)/\mathrm{d}\xi=2/3,\quad Re_x=u_e x/v_e,\\
&Ec=u_e^2/2H_e=2^{-1}(\gamma-1)M_e^2/[1+2^{-1}(\gamma-1)M_e^2],\\
&f(0,t^*)=A,\quad A=-(3/2)^{1/2}[(\rho w)_w/(\rho u)_e]Re_x^{1/2},\\
&\rho_e/\rho=h/h_e=(g-Ecf'^2)/(1-Ec),\\
&\mu/\mu_e=(h/h_e)^{\omega}=[(g-Ecf'^2)/(1-Ec)]^{\omega},\\
&N=\rho\mu/\rho_e\mu_e=[(g-Ecf'^2)/(1-Ec)]^{\omega-1}.
\end{aligned} \tag{8}$$

We use the transformations given in (8) and find (ρw) from (1) and use it along with (8) in (2)–(4). Consequently, we get the following semi-similar equations

$$(Nf'')'+(f+\alpha s)f''-\partial f'/\partial t^*=0, \tag{9}$$

$$(Ns'')'+(f+\alpha s)s''+\alpha(\rho_e/\rho-s'^2)+(2/3)(\rho_e/\rho-f's')-\partial s'/\partial t^*=0, \tag{10}$$

$$(Pr^{-1}Ng')'+(f+\alpha s)g'+Ec[(1-Pr^{-1})Nf'f'']'-\partial g/\partial t^*=0 \tag{11}$$

with boundary conditions

$$\begin{aligned}
&f(0,t^*)=A,\quad f'(0,t^*)=s(0,t^*)=s'(0,t^*)=0,\\
&g(0,t^*)=g_w(1+\epsilon),\\
&f'(\infty,t^*)=s'(\infty,t^*)=g(\infty,t^*)=1.
\end{aligned} \tag{12}$$

The initial conditions given by the steady-state equations which can be obtained from (9)–(11) by putting $t^*=\epsilon=\partial f'/\partial t^*=\partial s'/\partial t^*=\partial g/\partial t^*=0$ in them. The steady state equations are

$$(Nf'')'+(f+\alpha s)f''=0, \tag{13}$$

$$(Ns'')'+(f+\alpha s)s''+\alpha(\rho_e/\rho-s'^2)+(2/3)(\rho_e/\rho-f's')=0, \tag{14}$$

$$(Pr^{-1}Ng')'+(f+\alpha s)g'+Ec[(1-Pr^{-1})Nf'f'']'=0 \tag{15}$$

with boundary conditions

$$\begin{aligned}
&f=A,\quad f'=s=s'=0,\quad g=g_w\qquad \text{at } \eta=0,\\
&f'=s'=g=1\quad \text{as } \eta\to\infty.
\end{aligned} \tag{16}$$

It may be noted that the initial steady state equations (13)–(15) under conditions (16) are identical to those of Wortman [16] and for $N=\omega=Pr=1$, $Ec=A=0$ to those of Wu and Libby [13].

It may be noted that non-unique solutions exist for many important and interesting problems in fluid dynamics which are governed by boundary layer or Navier–Stokes equations [13,25–31]. However, in most cases, the physical significance of multiple solutions is uncertain. In these cases, the classical solutions have been obtained by solving the two-point boundary value problem numerically. For the second or multiple solutions different sets of initial profiles and the edge of the boundary layer (η_∞) are chosen. This procedure yields non-unique solutions. When suction or magnetic field or both are applied, the boundary layer becomes thin and it is not possible to get two or more independent sets of initial profiles which can yield two or more independent solutions of the same problem satisfying all the boundary conditions.

For the generalized vortex flow imposed over an infinite disk, King and Lewellen [32] and Stewartson and

Troesch [33] have found that no solution exists for the potential vortex flow in the absence of the magnetic field, but it exists if the magnetic parameter $M \geqslant 0.1$. Nanbu [34] has reported that the solution for the potential vortex flow in the absence of the magnetic field exists when the suction parameter $A \geqslant 1.74$. Since suction or magnetic field affects the existence of the solution, it is interesting to examine the role of suction on the non-uniqueness of the present problem. By increasing the value of the suction parameter from 0–2 (nearly), it is possible to show that only one solution is obtained numerically. However, this is not a mathematical condition for the uniqueness of the solution. More theoretical work is required to find the necessary and sufficient conditions for the uniqueness of the solutions of the boundary layer or Navier–Stokes equations [35]. This aspect will be considered in future.

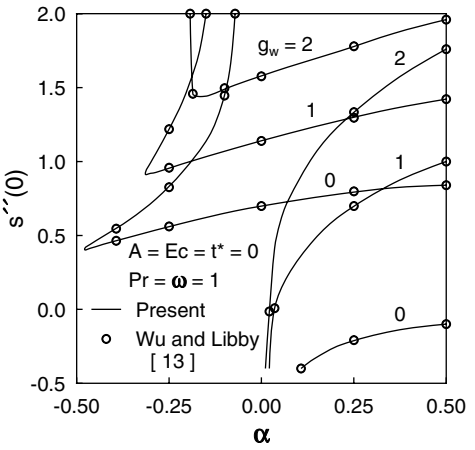

Fig. 2. Comparison of cross-flow surface shear stress for the steady flow ($s''(0)$), when $A = Ec = t^* = \epsilon = 0$, $Pr = \omega = N = 1$ with that of Wu and Libby [13].

3. Method of solution

Eqs. (9)–(11) under boundary conditions (12) and initial conditions (13)–(16) have been solved by an implicit finite-difference scheme in combination with the quasi-linearization technique [20,21]. First the non-linear equations (9)–(11) are linearized by using the quasi-linearization technique [20]. The resulting linear partial differential equations have been expressed in difference form by means of central-difference scheme in η-direction and backward-difference scheme in t^*-direction. These equations are then reduced to a system of linear algebraic equations with a block tri-diagonal structure and are solved by using Varga's algorithm [36]. The step sizes in η- and t^*-directions are chosen as $\Delta\eta = 0.05$ and $\Delta t^* = 0.001$ in the time interval $0 \leqslant t^* \leqslant 0.1$ and $\Delta t^* = 0.01$ for $t^* > 0.1$ and the edge of the boundary layer $\eta_\infty = 6$ for $A \geqslant 2$. In our analysis, we have taken $A \geqslant 2$ to ensure unique solution. These values are taken after carrying out the sensitivity analysis. A convergence criterion based on the relative difference between the current and the previous iterations is used. When this difference becomes 10^{-5}, the solution is assumed to have converged and the iterative process is terminated.

4. Results and discussion

Eqs. (9)–(11) under boundary and initial conditions (12)–(16) have been solved by using an implicit finite-difference scheme in combination with the quasi-linearization technique as described earlier. In order to assess the accuracy of our method, we have compared the surface shear stresses in the streamwise and cross-flow directions $(f''(0), s''(0))$ for $t^* = 0$ (initial steady state), $A = 0$ (without suction), $Ec = 0$ (without viscous dissipation), $Pr = 1$, $N = \omega = 1$ (constant density–viscosity product) with those of Wu and Libby [13] and found them in very good agreement. The comparison is shown in Figs. 1 and 2. We have also compared the ratio of the surface shear stresses and the heat transfer for the initial steady case $(f''(0)/f_0''(0),\ s''(0)/s_0''(0),\ g'(0)/g_0'(0))$ when $\omega = 0.5$, $g_w = 0.1$. $A = 0$, $Ec = 0.5$, $Pr = 0.715$ with those of Wortman [16]. The results are found to be in very good agreement. The maximum difference is found to be less than 1%. It is evident from Figs. 1 and 2 that the surface shear stresses $(f''(0), s''(0))$ for the steady-state case obtained by us for $A = 0$ (without suction) as well as by Wu and Libby [13] have two values in a certain range of cross-flow parameter α and this range reduces as the total enthalpy at the wall g_w increases.

The temporal development of the total enthalpy and velocity profiles $(g(\eta, t^*), f'(\eta, t^*), s'(\eta, t^*))$ and their gradients $(g'(\eta, t^*),\ f''(\eta, t^*),\ s''(\eta, t^*))$ for $A = 2$, $\omega = 0.5$, $M_e = 20$, $g_w = 0.5$, $\epsilon = 0.1$, $Pr = 0.7$, $\gamma = 1.4$, $\alpha = 0.5$ has been studied, but only the total enthalpy and its gradient are shown in Fig. 3. The effect is found to be more pronounced on the total enthalpy and its gradient and shows some interesting results. In small interval of time $0 < t^* < 0.01$, the total enthalpy of the fluid near the wall is less than that at the wall. The physical reason for this behaviour is that at time $t^* = 0$, the total enthalpy at the wall g_w ($g_w < 1$) is less than that of the surrounding fluid. At time $t^* > 0$, the total enthalpy at the wall is suddenly increased above that of the surrounding fluid near the wall. Hence for a small time interval, the total enthalpy of the fluid near the wall is less than that at the wall. In this case, the total enthalpy profiles $g(\eta, t^*)$ have a point of inflexion as evident from maximum in $g'(\eta, t^*)$. On the other hand, the velocity profiles in the streamwise direction $f'(\eta, t^*)$ have no point of inflexion, but the velocity profiles in the cross-flow direction $s'(\eta, t^*)$ near the wall

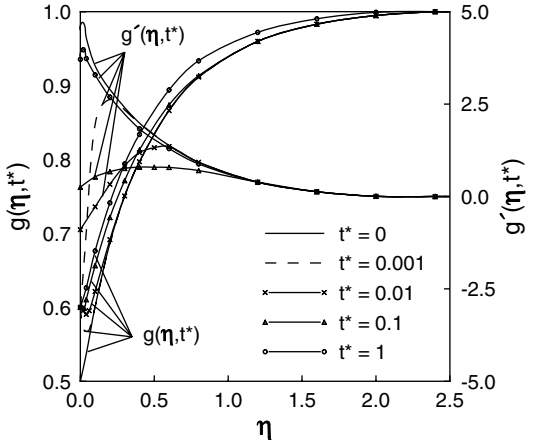

Fig. 3. Temporal development of the total enthalpy profile and its gradient $(g(\eta,t^*), g'(\eta,t^*))$ for $A = 2$, $\omega = g_w = \alpha = 0.5$, $\epsilon = 0.1$, $Pr = 0.7$, $\gamma = 1.4$, $M_e = 20$.

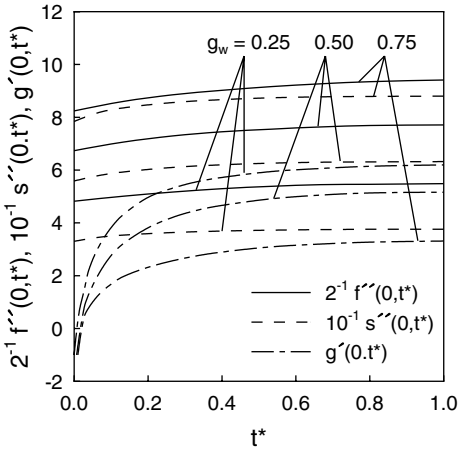

Fig. 4. Temporal development of the surface heat transfer $(g'(0,t^*))$ and streamwise and cross-flow surface shear stresses $(2^{-1}f''(0,t^*), 10^{-1}s''(0,t^*))$ for $A = 2$, $\omega = \alpha = 0.5$, $\epsilon = 0.1$, $Pr = 0.7$, $\gamma = 1.4$, $M_e = 20$.

have velocity overshoot (i.e., the velocity of the fluid near the wall exceeds that at the edge of the boundary layer) as evident from the minimum in $s''(\eta,t^*)$. This velocity overshoot occurs for all t^* when the cross-flow parameter $\alpha > 0$ (i.e., in the windward plane of symmetry). Since the perturbation in the total enthalpy at the wall is taken as small ($\epsilon = 0.1$), the changes in the velocity and temperature profiles and their gradients are small. If ϵ is increased, these changes will become more significant. Also, the surface shear stress increase with time due to the impulsive increase in the total enthalpy at the wall.

The effects of the total wall enthalpy g_w on the temporal development of the surface shear stresses in the streamwise and cross-flow directions $(f''(0,t^*), s''(0,t^*))$ and the surface heat transfer $(g'(0,t^*))$ for $A = 2$, $\omega = \alpha = 0.5$, $M_e = 20$, $\epsilon = 0.1$, $Pr = 0.7$, $\gamma = 1.4$ are presented in Fig. 4. For a fixed time, the surface shear stresses in the streamwise and cross-flow directions and the surface heat transfer $(f''(0,t^*), s''(0,t^*), g'(0,t^*))$ strongly depend on g_w and they increase with it except $g'(0,t^*)$ which decreases. The reason for this trend can be explained as follows. For gases increase in g_w implies reduction in the density of the gas. This causes reduction in momentum and thermal boundary layers. Consequently, the surface shear stresses increase with g_w, but the heat transfer decreases due to the reduction in the total enthalpy gradient. The surface shear stresses in the streamwise and cross-flow directions increase, respectively, by about 78% and 136%, when g_w increases from 0.25 to 0.75, but the heat transfer decreases by about 46%. For a given g_w, they increase with time t^*, however the effect is more pronounced on the heat transfer $(g'(0,t^*))$ than on the surface shear stresses, because step increase in the total enthalpy at $t^* > 0$ directly affects the heat transfer. At time $t^* = 0$, the heat transfer $g'(0,t^*) > 0$ which implies that the heat is transferred from the fluid to the wall. However at $t^* > 0$, the total enthalpy at the wall is increased and it becomes more than that of the fluid near the wall for a small time interval. Hence in that time interval, $g'(0,t^*) < 0$ indicating that the heat is transferred from the wall to the fluid. The shear stresses continuously increase with time and no such phenomenon is observed.

The effects of suction (A) on the surface shear stress in the streamwise direction and the surface heat transfer $(f''(0,t^*), g'(0,t^*))$ for $\omega = \alpha = g_w = 0.5$, $M_e = 20$, $\epsilon = 0.1$, $Pr = 0.7$, $\gamma = 1.4$ are displayed in Fig. 5. Since the effect of A on the cross-flow shear stress $(s''(0,t^*))$ is found to be very small, it is not shown in the figure. For a fixed time, the surface shear stress in the streamwise direction $(f''(0,t^*))$ and the surface heat transfer $(g'(0,t^*))$ significantly increase with A. For $t^* = 1$, $f''(0,t^*)$ and $g'(0,t^*)$ increase by about 100% as A increases from 2 to 4. The increase in suction causes thinner momentum and thermal boundary layers. Therefore, the surface shear stress in the streamwise direction and the surface heat transfer increase with A.

The effects of the cross-flow parameter α on the surface shear stress in the cross-flow direction $(s''(0,t^*))$ for $A = 2$, $g_w = \omega = 0.5$, $M_e = 20$, $\epsilon = 0.1$, $Pr = 0.7$, $\gamma = 1.4$ are shown in Fig. 6. Since the effects of α on the streamwise surface shear stress $(f''(0,t^*))$ and the heat transfer $(g'(0,t^*))$ are comparatively small, it is not shown here. For a fixed time t^*, the cross-flow shear stress $(s''(0,t^*))$ increases with α. For $t^* = 1$, it increases by about 182% as α increases from -0.5 to 1.0. On the other hand, the streamwise surface shear stress $(f''(0,t^*))$ and the surface heat transfer $(g'(0,t^*))$ increase by about 6%. Since positive α acts like favourable

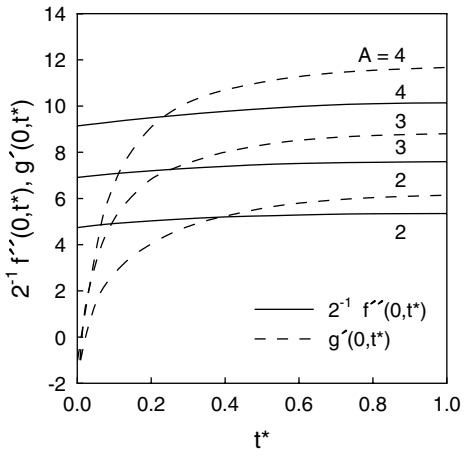

Fig. 5. Effects of suction A on the surface shear stress in the streamwise direction and the surface heat transfer ($2^{-1}f''(0,t^*)$, $g'(0,t^*)$) for $A = 2, 3, 4$, $g_w = 0.25$, $\omega = \alpha = 0.5$, $\epsilon = 0.1$, $Pr = 0.7$, $\gamma = 1.4$, $M_e = 20$.

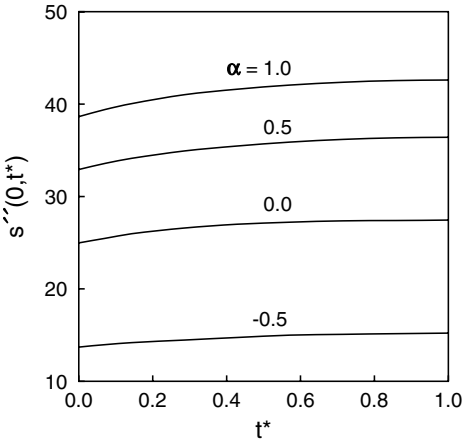

Fig. 6. Effects of the cross-flow parameter α on the cross-flow surface shear stress ($s''(0,t^*)$) for $\alpha = -0.5, 0, 0.5, 1.0$, $g_w = 0.25$, $\epsilon = 0.1$, $\omega = \alpha = 0.5$, $Pr = 0.7$, $\gamma = 1.4$, $M_e = 20$.

pressure gradient and negative α acts like adverse pressure gradient, its effect on the cross-flow shear stress is more significant than on the streamwise shear stress and the heat transfer.

5. Conclusions

One of the interesting results is that in a small time interval after the start of the impulsive change in the total enthalpy, the direction of the heat transfers changes. The surface shear stresses in the streamwise and cross-flow directions and the heat transfer increase with time and reach final steady state values rather quickly. Appreciable changes take place only in a small time interval after the impulsive increase in the total enthalpy. For a fixed time, the total enthalpy at the wall significantly increases the surface shear stresses in the streamwise and cross-flow directions, but the surface heat transfer decreases. On the other hand, the suction increases appreciably the surface shear stress in the streamwise direction and the surface heat transfer, whereas the cross-flow parameter increases significantly only the cross-flow shear stress. The application of suction enables us to obtain unique solution.

References

[1] J. Cousteix, Three-dimensional and unsteady boundary layer computations, Ann. Rev. Fluid Mech. 18 (1986) 173–196.
[2] R. Betters, J. Watts, A.A. Balkema, Unsteady Flow and Fluid Transients, Netherland Publishers, 1992.
[3] P.A. Libby, Heat and mass transfer at a general three-dimensional stagnation point, AIAA J. 5 (1967) 507–517.
[4] M. Kumari, G. Nath, Unsteady laminar compressible boundary-layer flow at a three-dimensional stagnation point, J. Fluid Mech. 87 (1978) 705–718.
[5] E. Reshotko, I.E. Beckwith, Compressible laminar boundary-layer over a yawed infinite cylinder with heat transfer and arbitrary Prandtl number, TN 1379, NACA, 1958.
[6] A. Sau, G. Nath, Unsteady compressible boundary-layer flow on the stagnation line of an infinite swept cylinder, Acta Mech. 108 (1995) 143–156.
[7] H.A. Dwyer, Some aspects of three-dimensional laminar boundary layers, Ann. Rev. Fluid Mech. 13 (1981) 217–229.
[8] F.K.Moore, Laminar boundary layer on circular cone in supersonic flow at small angle of attack, TN 2521, NACA, 1951.
[9] F.K. Moore, Laminar boundary layer at large angle of attack, TN 2844, NACA, 1952.
[10] E. Reshotko, Laminar boundary layer with heat transfer on a cone at angle of attack in a supersonic stream, TN 4152, NACA, 1957.
[11] J.W. Murdock, The solution of sharp cone boundary layer equations in the plane of symmetry, J. Fluid Mech. 54 (1972) 665–678.
[12] B. Roux, Supersonic laminar boundary layer near the plane of symmetry of a cone at incidence, J. Fluid Mech. 51 (1972) 1–14.
[13] P. Wu, P.A. Libby, Laminar boundary layer on a cone near a plane of symmetry, AIAA J. 11 (1973) 326–333.
[14] S.G. Rubin, T.C. Lin, F. Tarulli, Symmetry plane viscous layer on a sharp cone, AIAA J. 15 (1977) 204–211.
[15] A. Lin, S.G. Rubin, Three-dimensional supersonic viscous flow over a cone at incidence, AIAA J. 20 (1982) 1500–1507.
[16] A. Wortman, Heat and mass transfer on cones at angles of attack, AIAA J. 10 (1972) 832–834.
[17] H.S. Takhar, K. Yano, S. Nakamura, G. Nath, Unsteady compressible boundary layer in the stagnation region of a

sphere with a magnetic field, Arch. Appl. Mech. 67 (1997) 478–486.
[18] A. Sau, G. Nath, Unsteady compressible boundary layer flow at the stagnation point of a rotating sphere with an applied magnetic field, Arch. Mech. 49 (1997) 111–127.
[19] S.V. Subhashini, G. Nath, Self-similar solution of unsteady laminar compressible boundary layers in the stagnation region of two-dimensional and axisymmetric bodies, Acta Mech. 134 (1999) 135–145.
[20] J.R. Radbill, G.A. McCue, Quasilinearization and Nonlinear Problems in Fluid and Orbital Mechanics, Elsevier, New York, 1970.
[21] K. Inouye, G. Tate, Finite-difference version quasilinearization applied to boundary layer equations, AIAA J. 12 (1974) 558–560.
[22] A. Wortman, H. Ziegler, G. Soo-Hoo, Convective heat transfer at general three-dimensional stagnation point, Int. J. Heat Mass Transfer 14 (1971) 149–152.
[23] F.K. Moore, Three-dimensional boundary layer theory, Advances in Applied Mechanics, 4, Academic Press, New York, 1956, pp. 160–224.
[24] P.A. Libby, H. Fox, R.J. Sanator, J. Decarlo, Laminar boundary layer near the plane of symmetry of a hypersonic inlet, AIAA J. 1 (1963) 2732–2740.
[25] P.A. Libby, Heat and mass transfer at a general three-dimensional stagnation point, AIAA J. 5 (1967) 507–517.
[26] N.D. Nguyen, J.P. Ribault, P. Florent, Multiple solutions for flow between coaxial disks, J. Fluid Mech. 68 (1975) 369–388.
[27] P.J. Zandbergen, D. Dijkstra, Non-unique solutions of the Navier–Stokes equations for the Karman swirling flow, J. Eng. Math. 11 (1979) 167–188.
[28] M. Lentinu, H.B. Keller, The von Karman swirling flows, SIAM J. Appl. Math. 38 (1980) 52–64.
[29] D.B. Ingham, Non-unique solutions of the boundary layer equations for the flow near the equator of a rotating sphere, Acta Mech. 42 (1982) 111–122.
[30] P.K.H. Ma, W.H. Hui, Similarity solutions of the two-dimensional unsteady boundary layer equations, J. Fluid Mech. 216 (1990) 537–559.
[31] R. Nazar, N. Amin, I. Pop, Unsteady mixed convection near the forward stagnation point of a two-dimensional symmetric body, Int. Comm. Heat Mass Transfer 30 (2003) 673–682.
[32] W.S. King, W.S. Lewellen, Boundary layer similarity solutions for rotating flow with or without magnetic interaction, Phys. Fluids 7 (1964) 1674–1680.
[33] K. Stewartson, B.R. Troesch, On a pair of equations occurring in swirling viscous flow with an applied magnetic field, ZAMP 28 (1977) 951–963.
[34] K. Nanbu, Vortex flow over a flat surface with suction, AIAA J. 9 (1971) 1042–1043.
[35] V.A. Solonnikov, A.V. Kazhikhov, Existence theorem for equations of motion of a compressible viscous fluid, Ann. Rev. Fluid Mech. 16 (1981) 79–95.
[36] R.S. Varga, Matrix Iterative Analysis, second ed., Springer, Berlin, 2000, p. 223.